AIChE WILEY InterScience DISCOVER SOMETHING GREAT

BIOENGINEERING, FOOD, AND NATURAL PRODUCTS

Numerical and Experimental Study of a Natural Convection Thawing Process

A. Ousegui, A. Le Bail, and M. Havet
UMR GEPEA (UA CNRS 6144-SPI). ENITIAA. Rue de la Géraudière BP 82225, 44322, Nantes Cedex 3, France

DOI 10.1002/aic.11035
Published online October 31, 2006 in Wiley InterScience (www.interscience.wiley.com).

The thawing process is a unit operation that exposes the food to risk of microbial growth. To evaluate this risk, numerical modelling is very useful. The thawing process by means of a 3-D numerical model is investigated. Both heat diffusion with phase change inside the product and on the convection phenomenon in the heating medium is focused on. This coupled model does not require an a priori *knowledge of the convective heat-transfer coefficient. The corresponding highly nonlinear equations were solved using a CFD software. Experimental investigations were carried out on a high-pressure vessel (temperature measurements), and on a specific device (velocity measurements). Comparisons between experimental and numerical results were very satisfactory, especially for transient temperature predictions. The model could then be exploited to assess process modification, and could be extended to investigate innovative processes at high-pressure.* © 2006 American Institute of Chemical Engineers *AIChE J,* 52: 4240–4247, 2006

Keywords: phase change, heat transfer, natural convection, CFD, PIV

Introduction

The processes based on phase change (freezing or thawing) take an important place in the food industry chain. The thawing process is maybe the more embarrassing process for the food industry. In fact, this process is considered as a "no added value" unit operation. During this long process, the food is exposed to risk of oxidation and cross contamination. If the thawing operation is not properly managed, it can be accompanied by undesirable modifications of texture, color or savor. It can also lead to a more important problem: a microbial development more especially at the surface of the food. Modeling the thawing process can be useful to predict the time-temperature history, and then the risk of microbial growth.

Among the novelty thawing food processes, high-pressure treatments are promising. For a thawing process at 200 MPa, phase transition of water occurs at -20°C. By combining low-temperature, and very-high-pressure, the microbial risk is considerably reduced. Otero et al[1] confirmed that the modification of the phase-change temperature with the pressure reduced the thawing time, and was accompanied by other positive effects like the inactivation of micro-organisms.

During high-pressure processes, the food is placed in a vessel, where it is compressed to the desired pressure level and maintained until the end of the treatment. Water is commonly used as compression fluid. However, there is a lack of knowledge concerning the internal temperatures of the food and the velocity field of the heating medium during this batch process. This is simply due to the technical difficulties of measurements in a high-pressure vessel.

The predictions of the evolution of the temperature field in the food are essential to ensure an optimal treatment and to adjust the process conditions. When a liquid is used as heat transferring medium (most of the time water), natural or mixed convection develops in the fluid, due to the temperature difference between the fluid and the product. The analysis of the velocity field in the fluid, and the transfer between this fluid and the product is essential for the optimization of

Correspondence concerning this article should be addressed to M. Havet at havet@enitiaa-nantes.fr.

the thawing time and for the improvement of the process (uniformity of heat treatment for example).

To perform a consistent heat-transfer study, two main phenomena should be modeled, the phase transitions inside the product and the convective flow in the enclosure. This article presents a preliminary approach carried out at atmospheric pressure. The main objective of this work consisted in modeling the phase transitions and the flow field occurring in an enclosure, which geometry was similar to a high-pressure vessel. We assessed our model in a specific configuration: the thawing of a rectangular slab immersed in a cylindrical enclosure. An experimental setup was also built in order to validate the model.

The mathematical formulation applied to phase change phenomena implies a complex situation of heat transfer (Stefan problem). Literature is rather abundant on analytical models developed to solve the Stefan problem. Crank[2] was among the firsts who applied the enthalpy method to model the solidification of a square cylinder of a fluid, with a surface temperature lowered at a constant rate. The enthalpy formulation of the Stefan problem was regularly improved for one-dimensional (1-D) space[3] the model allowed tracking the moving boundary continuously in time, and determining the temperature profiles at each time-step. Analytical solutions in one dimension were extended by Ramos et al.[4] to consider power-law functions of temperature for both thermal conductivity and specific heat. Whatever the extension of these analytical solutions, they are restricted to simple configurations, and numerical methods are required to consider for example the dependence of food properties to the temperature. Finite volume schemes are basically used; they provided a good agreement with experimental data in regular geometrical shapes, but for realistic food geometries (irregular forms) Agnelli and Mascheroni[5] showed that they were not adapted. The Galerkin finite element method was also employed to obtain solutions for phase change in 1-D slabs of pure material. Bhattacharya et al.[6] demonstrated the ability of the method to efficiently capture multiple thawing fronts. The freezing and thawing processes of frozen food were analyzed with a similar model by Huan et al.[7] They pointed out the strong influence of the velocity and temperature of the freezing medium (air) on the freezing rate.

All works presented earlier considered only the heat transfer in the solid domain. Very little effort has been made so far on the coupled heat transfer between the solid and the fluid domain in the case of natural convection. In most available studies, a fixed convective heat-transfer coefficient was assumed between the fluid and the solid domain. This assumption is no more valid for large products immersed in a heating medium. In these conditions the temperature gradient along the surface tends to modify the heat transfer.[8]

The scientific objective of this article is to investigate experimentally and numerically the food thawing process at atmospheric pressure, taking into account:

(a.) the dependence of properties of food on temperature,

(b.) the temperature field and ice quantity distribution in the product,

(c.) the transient evolution of the local convective heat-transfer coefficient,

(d.) the velocity and temperature fields of the thawing medium.

A 3-D model accommodating transient-convective heat-transfer between a frozen food solid and a fluid placed in an enclosure was developed. The model was tested and compared with experimental results at pilot scale, including transient temperature evolution, and PIV measurement of velocity in the surrounding of the solid domain. This experimental technique already proved its efficiency to analyse flows of this nature.[9]

Materials and Methods

Tylose (methylcellulose gel) was used as a food model with a water content equal to 764 g water/kg. Tylose slabs were provided by MADI S.n.c. (MADI — Italy). The dimension of tylose slabs used for the experiments was 100 $\times$ 200 $\times$ 25 mm. Slabs were vacuum packed in a polyethylene bag. Afterwards, thermocouples were installed in the slabs using sealed passages.

Experimental setup

Temperature Measurements. The vessel had an inner diameter of 120 mm and an internal height of 300 mm. It was made of stainless steel and was in fact designed to process under high-pressure conditions. It was kept at constant temperature and was circulated by a temperature-controlled fluid (Figure 1). The tylose slabs were installed at the center of the vessel (Figure 2) equipped with an instrumented obturator allowing the passage of five calibrated thermocouples. Three thermocouples (K-type, $\oslash$ 1 mm) were positioned trough x direction at the center ($x = 0$; $r = 0$; $z = 15$ cm), at the middle ($x = 0$; $r = 0.62$; $z = 15$ cm), and at the surface of the sample ($x = 0$; $r = 1.25$ cm; $z = 15$ cm). Two other thermocouples ($\oslash$ 0.3 mm, K-type) were installed in upper ($x = 0$; $r = 0$; $z = 28$ cm) and lower ($x = 0$; $r = 0$; $z = 3$ cm) locations of the vessel.

A data logger (SA32, AOIP) was used to record the temperature. The thermocouples were calibrated against a refer-

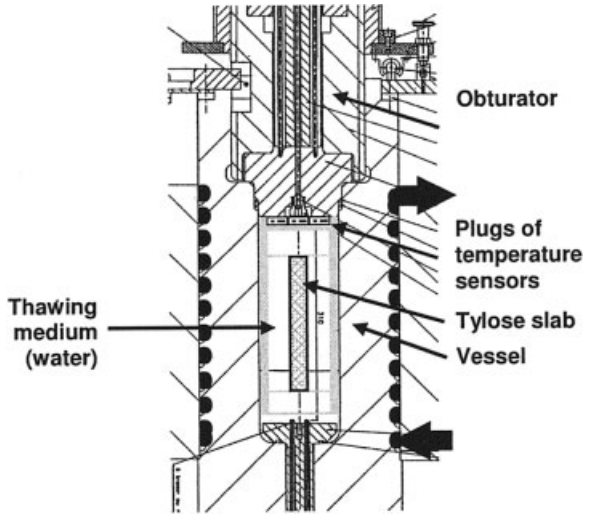

Figure 1. HP vessel used for temperature measurements.

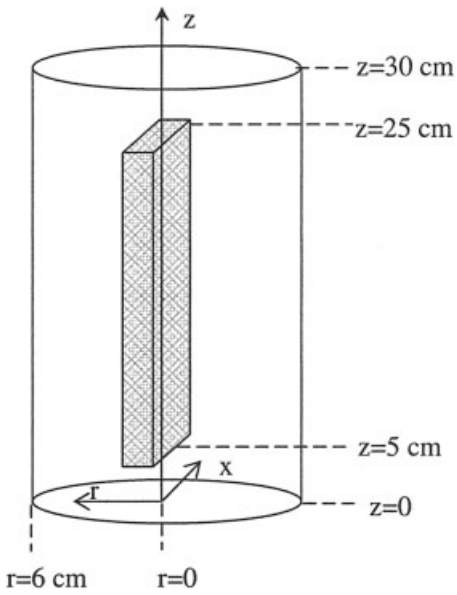

Figure 2. The geometry considered: a slab installed in a cylindrical vessel.

ence platinum temperature probe (Comptoir Lyon Allemand – Lyon – France). The accuracy of temperature measurements was of /– 0.3°C. Data logger loaded temperature every 5 s during thawing experiments.

Fluid velocity measurements

The flow pattern was studied in a specific transparent experimental device made out of Plexiglas. This experimental device reproduced the geometry of the vessel, and of the slab of frozen tylose with a 1/1 scale dimension. A cylindrical enclosure reproducing the inner dimensions of the vessel was placed in a parallelepiped box (height × width × thickness: 300 mm × 300 mm × 350 mm). Water was circulated inside this parallelepiped box, making it possible to maintain the external wall temperature of the cylinder at 20°C. One of the vertical side walls of the parallelepiped was covered with a black painted aluminium plate to allow PIV measurements. A hollow brass box with dimensions similar to that of the tylose slab was used to simulate the slab of frozen tylose. A flow of a temperature-controlled water-glycol mixture in this brass slab box maintained its temperature at 5°C. In the system (Figure 3), one can distinguish the brass slab painted in black to avoid light reflexion during PIV measurements.

A continuous Argon Ion laser, emitting at a wavelength of 488 nm, was used for PIV measurements. Two windows were considered for the PIV measurements (height × width = 80 mm × 60 mm). A double image 700 video camera was used (Dantec 80C42 – Denmark); it was equipped with a CCD sensor with a maximum resolution of 768 × 484 pixels. To visualize the natural convection flow patterns, the "single frame" method was selected at a frequency of 4 Hz. Titane Dioxyde (TiO_2) particles with 5-30 μm dia. usually used in PIV experiments, were adopted.

Mathematical Model

As the thawing medium was water, it was considered as a Newtonian and incompressible fluid. Continuity (Eq. 1), momentum (Eq. 2) and energy (Eqs. 3, 4) equations were considered, taking into account natural convection terms and applying Boussinesq approximation (Eq. 5). All thermo-physical and hydrodynamic properties of this medium were supposed to be constant.

$$\vec{\nabla}\vec{V} = 0 \tag{1}$$

$$\rho\left(\frac{\partial\vec{V}}{\partial t} + \vec{V}\cdot\vec{\nabla}\vec{V}\right) = \mu\nabla^2\vec{V} - \vec{\nabla}p + \rho\vec{g} \tag{2}$$

$$\rho\frac{\partial H_{water}}{\partial t} + \rho\vec{V}\cdot\vec{\nabla}H_{water} = \vec{\nabla}\cdot(\lambda\vec{\nabla}T) \tag{3}$$

$$H_{water}(T) = \int C_p(T)\mathrm{d}T \tag{4}$$

$$\rho = \rho_{T_0}\cdot(1-\alpha(T-T_0)) \tag{5}$$

For the solid domain, the physical model of Cleland and Earle,[10] based on apparent specific heat was used (Eq. 6). Additive equations, based on the contribution of each component (water, ice and fibers), were used to evaluate the specific heat capacity and thermal conductivity. Some measurements using standard methods (DSC, hot wire) were also carried out to validate these expressions.

The Miles method described by Otero et al.[1] and Ousegui[11] was adopted to calculate the ice quantity (Eq. 7). Like Cogné et al.[12] and Maroulis et al.[13], a classical parallel model was adopted for the apparent specific heat capacity (Eq. 8) and a Krisher model based on combination between parallel and serial models was used for thermal conductivity (Eq. 9).

$$\rho(C_p)_{\mathrm{app}}\frac{\partial T}{\partial t} = \nabla\cdot\left(\lambda^t_{\mathrm{tylose}}\nabla T\right) \tag{6}$$

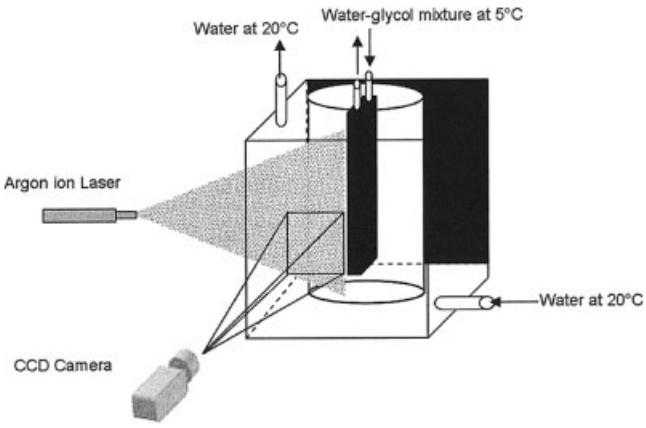

Figure 3. Experimental setup for PIV measurement.

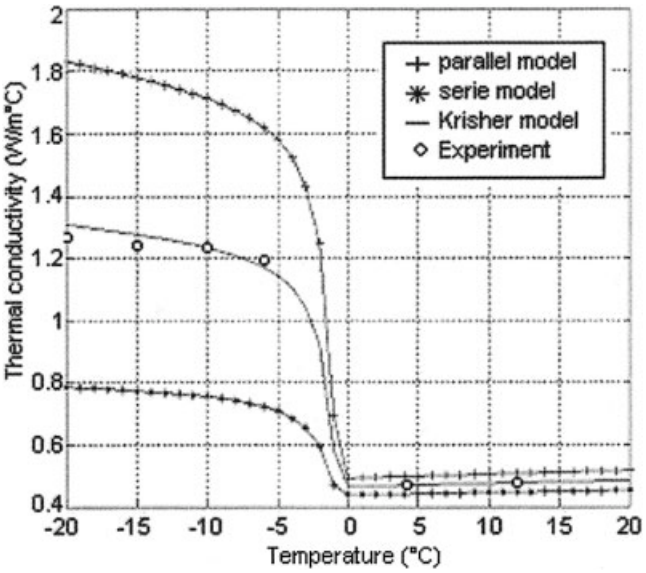

Figure 4. Thermal conductivity of tylose, experimental data and calculated result.

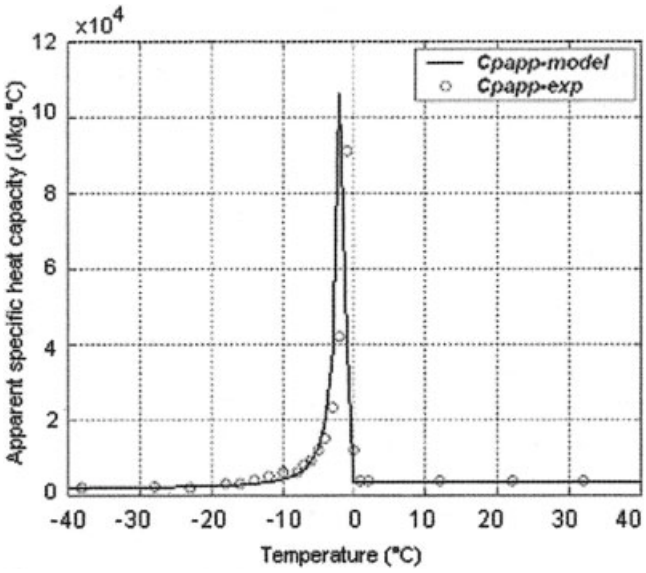

Figure 5. Apparent specific capacity of tylose, experimental data and calculated results.

$$X_{\text{ice}} = (X_{\text{wt}} - X_b) \cdot \left(1 - \frac{T_f}{T}\right) \tag{7}$$

$$(Cp)_{\text{app}} = \sum_j X_j C_{\text{pj}} + L\frac{dX_{\text{ice}}}{dT} \tag{8}$$

$$\lambda(T) = \frac{1}{\frac{0.5}{\lambda^{\text{para}}(T)} + \frac{0.5}{\lambda^{\text{serie}}(T)}} \tag{9}$$

The comparison between numerical and experimental results for apparent specific heat capacity and thermal conductivity (Figures 4 and 5) confirmed the adequacy of these expressions. The conservation of the heat flux was applied at the interface between the solid and the liquid (Eq. 10).

$$-\lambda S\vec{\nabla}T \cdot \vec{n} = hS(T_{\text{liquid}} - T_{\text{solid}}) \tag{10}$$

Numerical model

The thawing medium was considered initially stagnant at a constant temperature (20°C). The initial temperature of the frozen tylose, deduced from the experiments, was fixed at −17°C. The temperature of the walls was fixed at 20°C. A quadrant of the geometry was considered for obvious symmetry reasons.

This model was performed using a CFD code (CFX.5-7), enhanced by specific subroutines for the thermophysical properties. The equations were solved using the coupled solution of Rhie and Chow,[14] with a second-order upwind-scheme for spatial discretisation and a second-order scheme for time.[15]

Triangular nonstructured technique was adopted for meshing the geometry (Figure 6). In order to well predict the heat transfer, the mesh was inflated at the interface between water and tylose (Figure 7).

Results: Temperature Field

Validation

Experimental and numerical temperature evolutions in the tylose slab are compared in Figure 8. The good agreement between the model and the experiment highlighted the ability of the model to simulate the thawing of tylose at atmospheric pressure. The thawing process is characterized in the core of the product by three main stages:

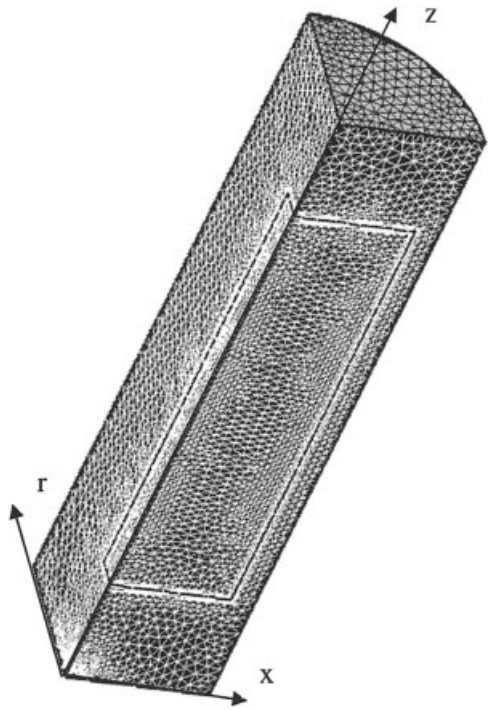

Figure 6. Volumetric mesh (1/4 of the volume).

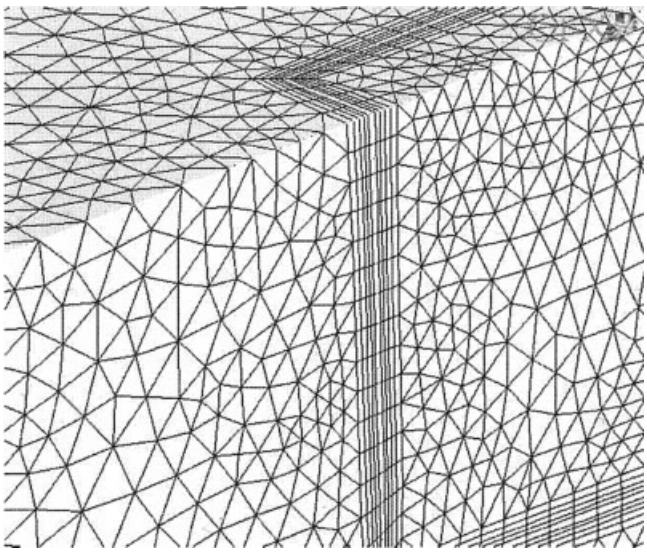

Figure 7. Refinement of the volumetric mesh close to the interface.

1st stage: fast increase of the temperature, until approaching the melting point (until t $\approx$ 400 s), 2nd stage: very slow temperature rise until crossing the initial freezing temperature ($t \approx$ 2000s). During this stage, the total absorption of the latent heat of melting occurs, which explains the quasi-stability of the temperature around the melting point.

3rd stage: fast increase of the temperature towards the ambient temperature.

At the interface ($r = 1.25$ cm), a fast temperature increase was observed until reaching ambient temperature, without temperature dwell during phase change. This phenomenon is commonly attributed to the high-convective heat transfer between the water and the tylose slab, supported by a great temperature difference ($\Delta T \approx 37^{\circ}$C).

Figure 9 presents the comparison between the experimental and the numerical evolution of the temperature of water respectively at the bottom and top locations inside the vessel. The decrease of temperature observed at the beginning of the process (first 200s) was followed by an increase of the temperature until reaching the ambient temperature fixed at 20°C. Temperature changes were larger in the lower part of the vessel. At this location, the cooling of water reached 6°C (modeling results), while it did not exceed 1.5°C at the top location. This difference was attributed to the development of a thermal-boundary layer, and to the fact that the cold fluid of higher density tends to accumulate in the lower part of the vessel.

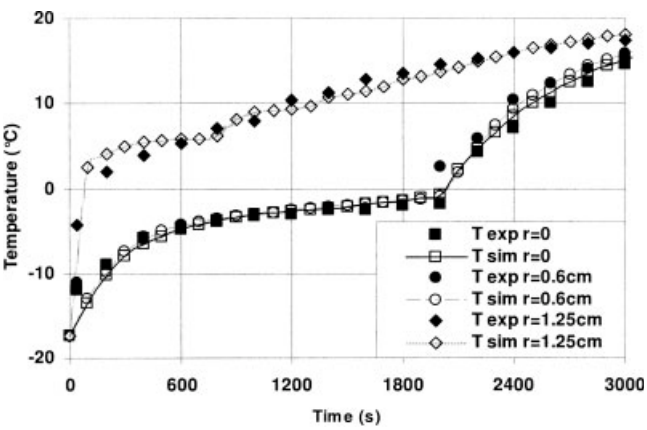

Figure 8. Temperature evolution in the tylose slab: experimental and simulation results.

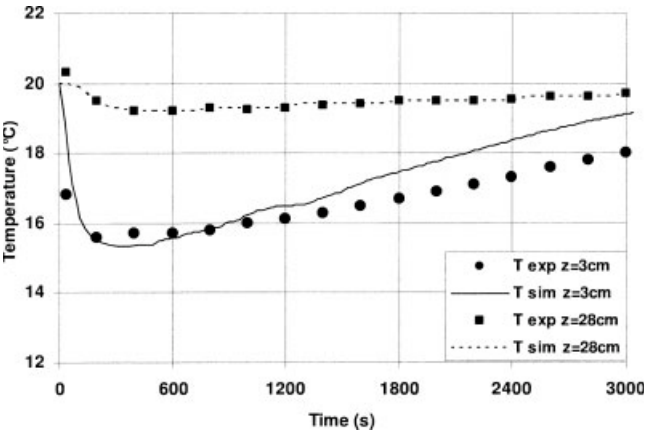

Figure 9. Temperature evolution at the top (z = 28 cm) and bottom (z = 3 cm) in the thawing medium (water): experimental and simulation results.

A fairly good agreement was observed between numerical and experimental results, despite the experimental difficulties. For example, initial conditions considered in the model, such as a uniform temperature or a zero velocity did not exactly reproduce the experimental conditions. We also imposed a constant temperature on the walls of the vessel, but this boundary condition could not be exactly guaranteed on all walls, especially at the top and bottom of the vessel. Other

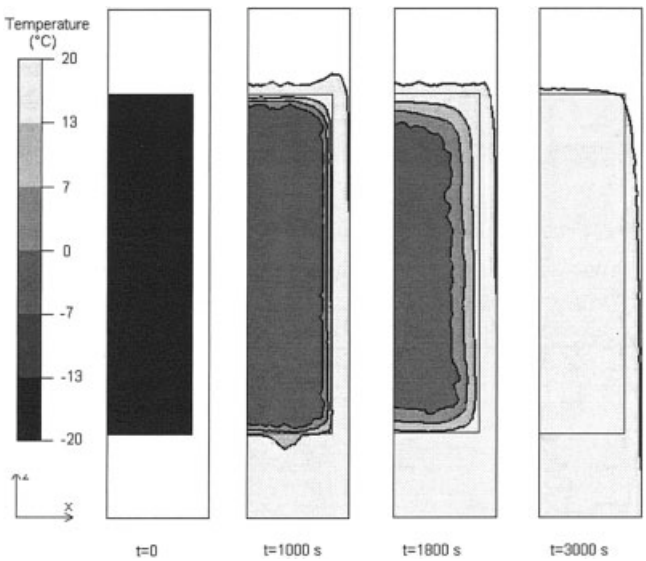

Figure 10. Evolution of the temperature in the tylose slab at r = 0 (simulation results).

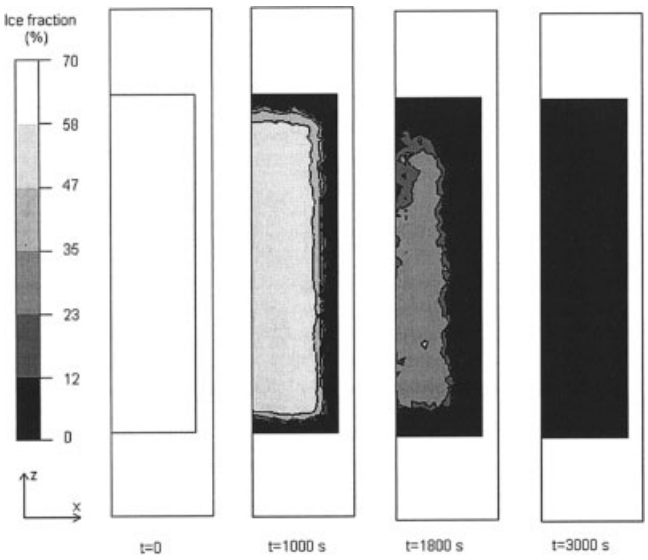

Figure 11. Evolution of the ice fraction in the tylose slab at *r* = 0 (simulation results).

parameters such as the expansion-contraction phenomenon related to the phase change were impossible to accommodate with a high-accuracy.

Natural convection effects

The transient evolutions of the temperature and ice quantity in the product were numerically predicted (Figures 10 and 11). The advance of the thawing front from the surface towards the center of the tylose slab could be easily pointed out in these figures. They also revealed that the higher-part of the product was thawed more quickly than the lower-part. This was well highlighted in Figure 11 (t = 1800s), where the ice, that was fully thawed at top location of the slab, was still present at the bottom of the tylose slab. This fact was attributed to the natural convection contribution; more precisely to the evolution of the temperature in water during the thawing process (as indicated in Figure 9). It showed that denser water tended to accumulate at the bottom of the vessel, resulting in a reduced heat-transfer rate.

Results: Velocity Field

The velocity field was experimentally investigated in stationary regime in the transparent experimental setup in the plane $x = 0$. The brass slab simulating the frozen tylose was maintained at constant temperature (5°C), and was immersed in the cylindrical enclosure. Water contained in the cylinder was maintained at 20°C. It was expected that the temperature difference between the slab surface, and the inner wall would generate a natural convection flow.

This flow pattern was numerically predicted as foreseen (Figure 12a). A downward boundary layer developed along the cold wall with a maximum velocity close to 1 $cm.s^{-1}$ at the trailing edge of the boundary layer. The water is relatively stagnant in the higher part of the enclosure, most of the fluid velocities are in the range of 1 $mm.s^{-1}$. The simulations revealed an intense zone of recirculation in the lower part of the vessel.

The velocity field obtained by PIV corroborated these results (Figure 12b). It also pointed out the flow going down along the cold wall, the recirculation in the lower part and the upward directed boundary layer along the hot wall.

A deeper analysis was done by comparing the experimental and numerical vertical velocity components at selected locations along the vertical axis. It should be noticed that we observed during the experiments a sedimentation of the particles and a quite inconsistent behaviour of the flow in the lower part of the vessel. This typical problem encountered in laminar natural convection lead us to focus on velocity profiles from z = 10 cm (Figure 13). These velocity profiles confirmed the two boundary layer flows and the stagnant zone in the core of the fluid. These comparisons indicated

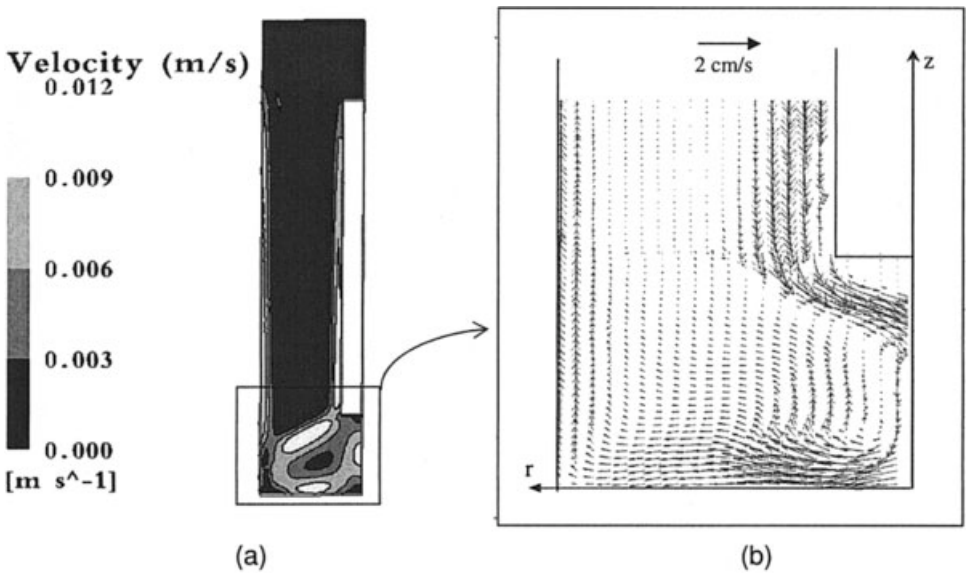

Figure 12. Velocity field (a): simulation results, (b) experimental data.

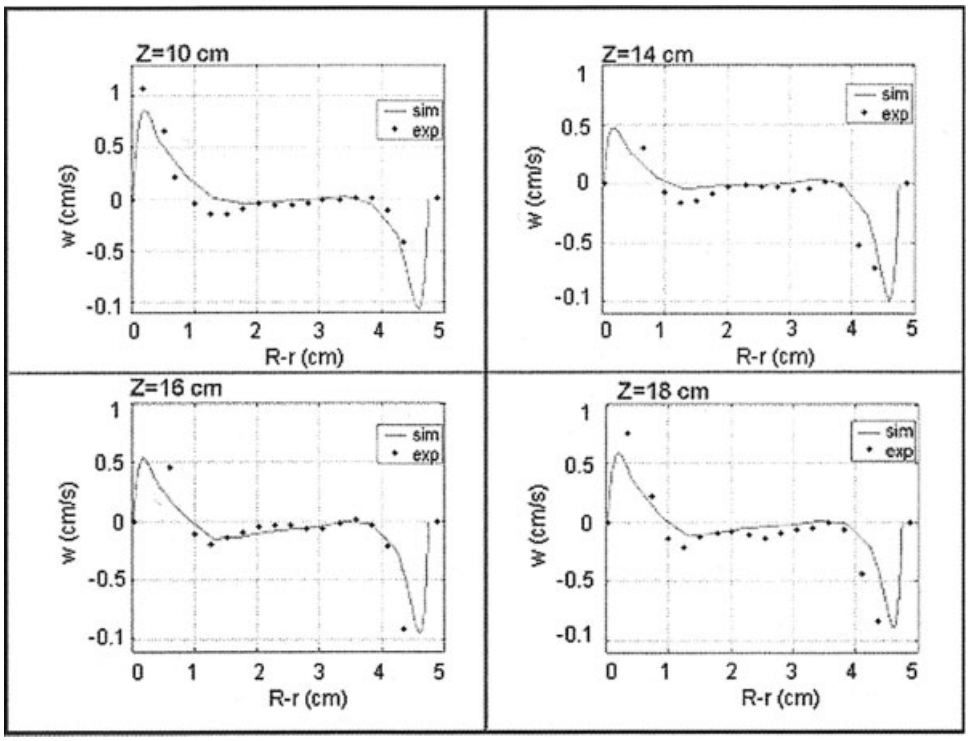

Figure 13. Velocity profiles (z component) between heat and cold walls at different heights (— simulation results; ● experimental data).

that the model was able to predict with a satisfactory agreement the velocity profiles, taking into account the fact that the analysis by PIV of the natural convection flow pattern remained a difficult task.

These velocity profiles confirmed the development of the two hydrodynamic boundary layers. Along the cold wall, the maximum of velocity was up to 1 $cm.s^{-1}$, whereas it ranged between 0.5 and 0.8 $cm.s^{-1}$ for the hot wall. These evolutions are primarily due to the driving force in natural convection, the temperature difference between the fluid and the wall. Figure 14 presents these temperature profiles at different heights obtained from simulation. It appeared that the temperature gradient along the cold wall was greater (11°C) than along the hot one (the gradient did not exceed 4°C).

Conclusion

A model has been developed to simulate the thawing process of a frozen tylose slab immersed in water in a cylindrical enclosure at atmospheric pressure. The phase change occurring inside the product was modeled using the apparent heat capacity method. Natural convection was considered applying Boussinesq approximation. It is noticeable that the predictions of the temperature evolution were in good agreement with experimental data both inside the product and inside the fluid. The main heat-transfer phenomena were well taken into account in the model.

The analysis of the velocity field in the thawing medium was fruitful. Results revealed the development of a downward boundary layer along the product and the establishment of a recirculation zone at the bottom of the vessel. The validation of the velocity field on a pilot scale in a steady case confirmed the ability of the model to predict natural convection effects. The model was also useful to bring information on the thawing front advance and on the heterogeneity of the treatment. Further works concern the extension of the model to high-pressure conditions.

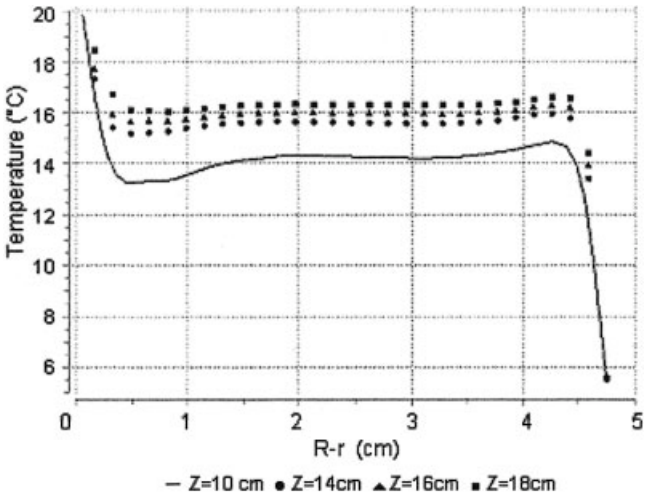

Figure 14. Temperature profiles between heat and cold walls at different heights (simulation results).

Acknowledgments

This study was partially funded by the European Project of Safe Ice (QLK1-CT-2002-02230) J. Pruvost, L. Guihard, and J. Laurenceau are thanked for their technical support during experimental work.

Notation

Roman letters

Cp = specific heat capacity, $J \cdot kg^{-1} \cdot K^{-1}$
$\vec{g}$ = gravity, $m \cdot s^{-2}$
h = convective heat transfer coefficient, $W \cdot m^{-2} \cdot K^{-1}$
t = time, s
T = temperature, K
p = Pressure, Pa
w = vertical velocity component, $m \cdot s^{-1}$
x, r, z = coordinates, m
S = surface, m^2
R = radius of the cylindrical vessel, m
$\vec{V}$ = velocity vector, $m \cdot s^{-1}$

Greek symbols

α = coefficient of thermal expansion, K^{-1}
ρ = density, $kg \cdot m^{-3}$
μ = dynamic viscosity, Pa·s
λ = thermal conductivity, $W \cdot m^{-1} \cdot K^{-1}$

Subscript

0 = initial condition
app = apparent
wt = total water content
f = freezing
b = bounded water

References

1. Otero L, Ousegui A, Guignon B, Le Bail A, Sanz P. Evaluation of the thermophysical properties of tylose gel under pressure in the phase change domain. *Food Hydrocolloids*. 2006;20:449–460.
2. Crank J. *Free and Moving Boundary Problems*. Oxford; Cambridge University Press; 1984.
3. Voller VR, Cross M. Use of enthalpy method in the solution of Stefan problems. *Numerical Methods in Heat Transfer*. 1981:177–200.
4. Ramos M, Cerrato Y, Gutierrez J. An exact solution for the finite stefan problem with temperature-dependent thermal conductivity and specific heat. *Int J Refrigeration*. 1994;17;2:130–134.
5. Agnelli M, Mascheroni R. Cryomechanical freezing. A model for the heat transfer process. *J of Food Eng*. 2001;47;4:263–270.
6. Bhattacharya M, Basak T, Ayappa KG. A fixed-grid finite element based enthalpy formulation for generalized phase change problems: role of superficial mushy region *International J of Heat and Mass Transfer*. 2002;45;24:4881–4898.
7. Huan Z, He S Ma Y. Numerical simulation and analysis for quick-frozen food processing. *J of Food Eng*. 2003;60;3:267–273.
8. Havet M, Blay D. Natural convection over a non-isothermal vertical plate. *Int J of Heat and Mass Transfer*. 1999;42;16:3103–3111.
9. Scanlon TJ, Stickland MT. An experimental and numerical investigation of natural convection melting. *Int Communications in Heat and Mass Transfer*. 2001;28;2:181–190.
10. Cleland AC, RL Earle. Assessment of freezing time prediction methods. *J of Food Sci*. 1984;49:1034–1042.
11. Ousegui A. Traitement Haute-Pression - Basse température: étude des phénomènes de transfert. University of Nantes, France; 2005. PhD Thesis.
12. Cogné C, Andrieu J, Laurent P, Besson A, Nocquet J. Experimental data and modeling of thermal properties of ice creams. *J of Food Eng*. 2002;58:331–341.
13. Maroulis ZB, Krokida M, Rahman MS. A structural generic model to predict the effective thermal conductivity of fruits and vegetables during drying. *J of Food Eng*. 2002;52;1:47–52.
14. Rhie CM, Chow WL. Numerical study of the turbulent flow past an airfoil with trailing edge separation. *AIAA J*. 1983;21;11:1525–1532.
15. Patankar SV. Numerical Heat Transfer and Fluid Flow. New York: Hemsisphere Publishing Corp; 1980.

Manuscript received Apr. 10, 2006, and revision received Jun. 16, 2006, and final revision received Sept. 22, 2006.